Supplementary Material (ESI) for Dalton Transactions

Supporting information

Construction of noninterpenetrating and interpenetrating Co(II) networks with halogenated carboxylate modulated by auxiliary N-donor coligands: structural diversity, electrochemical and photocatalytic properties

Shao-Yun Hao[a], Suo-Xia Hou[a], Kristof Van Hecke[b], Guang-Hua Cui[a]

[a]*College of Chemical Engineering, Hebei Key Laboratory for Environment Photocatalytic and Electrocatalytic Materials, North China University of Science and Technology, Tangshan Hebei 063009, P. R. China*

[b]*XStruct, Department of Inorganic and Physical Chemistry, Ghent University, Krijgslaan 281-S3, 9000 Ghent, Belgium*

Corresponding author: Guang Hua Cui

Fax: +86-0315-2592170. Tel: +86-0315-2592169.

E-mail: tscghua@126.com

S1 Electrochemical experiment

CP **1** bulk-modified carbon paste electrode (1-CPE) was fabricated as follows: 0.05 g of graphite powder and 0.015 g of CP 1 were mixed and ground together with an agate mortar and pestle to achieve an even mixture, and then 0.02 mL of Nujol was added with stirring. The homogenized mixture was packed into a glass tube with 3 mm inner diameter to a length of 8 mm, and the tube surface was wiped with weighing paper. Electrical contact was established with a copper wire. The same procedure was used for the preparation of bare CPE and 2–6-CPEs.

Table. **S1** Crystal and refinement data for CPs **1**–**3** and **4**–**6**.

Table. **S2** Selected bond lengths [Å] and angles [°] for CPs **1**–**6**.

Fig. S1 The IR spectra of the powder of the CPs **1**–**6** after catalytic experiments.

Fig. S2 The simulated from single-crystal data and obtained from the experiments X-ray powder diffraction patterns of CPs **1**–**6.**

Fig. **S3a** Cyclic voltammograms of **1**-CPE in 1 M H_2SO_4 solution at various scan rates (from inner to outer: 20, 60, 100, 120, 140, 160, 180 mV s^{-1}).

Fig. **S3b** Cyclic voltammograms of **5**-CPE in 1 M H_2SO_4 solution at various scan rates (from inner to outer: 20, 60, 100, 120, 140, 160, 180 mV s^{-1}).

Fig. **S4** UV−vis absorption spectra at room temperature and main absorption bands for the N-donor ligands, H_2DCTP ligand, and CPs **1**–**6**.

Fig. **S5** Absorption spectra of the MB solution during the decomposition reaction under UV irradiation with the presence of CPs **2**–**6**.

Fig. S6 X-ray powder diffraction patterns of CPs **1**–**6** after catalytic experiments.

Fig. S7 Three cycling runs of CPs **1**–**6** in the degradation of MB solution.

Table S1a Crystal and refinement data for CPs **1**–**3**

CPs	**1**	**2**	**3**
Chemical formula	$C_{26}H_{20}Cl_2CoN_4O_4$	$C_{30}H_{26}Cl_2CoN_4O_4$	$C_{32}H_{24}Cl_2CoN_4O_4$
Formula weight	582.29	636.38	658.38
Crystal system	Triclinic	Monoclinic	Monoclinic
Space group	*P***Error!**	*C2/c*	*P2(1)/c*
a (Å)	9.811(5)	20.910(3)	9.7424(7)
b (Å)	10.140(5)	11.6409(15)	16.9341(13)
c (Å)	13.189(7)	12.3090(16)	18.1411(13)
α (°)	82.569(8)	90	90
β (°)	70.262(7)	116.005(2)	98.617(2)
γ (°)	87.657(7)	90	90
V (Å^3)	1224.7(11)	2692.7(6)	2959.1(4)
Z	2	4	4
D_{calcd} (g/cm^3)	1.579	1.570	1.478
Absorption coefficient, mm^{-1}	0.961	0.882	0.805
F(000)	594	1,308	1,348
Crystal size, mm	0.27 x 0.26 x 0.23	0.24 x 0.22 x 0.20	0.26 x 0.22 x 0.21
θ range, deg	1.653 - 27.531	2.058 - 27.467	2.547 - 28.310
Index range *h*, *k*, *l*	-11/12, -11/13, -12/17	-27/27, -15/12, -15/15	-12/13, -22/22, -24/22
Reflections collected	7,402	8,088	83,301
Independent reflections (R_{int})	5,363 (0.0378)	3,051 (0.0479)	7,327 (0.0503)
Data/restraint/parameters	5,363/0/334	3,051/0/188	7,327/0/390
Goodness-of-fit on F^2	0.970	1.032	1.116
Final R_1, wR_2 ($I > 2\sigma(I)$)	0.0592, 0.1452	0.0430, 0.0919	0.0556, 0.1227
Largest diff. peak and hole	0.595, -0.846	0.326, -0.335	0.530, -0.474

Table S1b Crystal and refinement data for CPs **4**–**6**

CPs	**4**	**5**	**6**
Chemical formula	$C_{96}H_{76}Cl_6Co_3N_{12}O_{14}$	$C_{47}H_{41}Cl_2CoN_6O_4$	$C_{34}H_{28}Cl_2CoN_4O_4$
Formula weight	2011.17	883.69	686.43
Crystal system	Monoclinic	Monoclinic	Monoclinic
Space group	*I2/a*	*I2/c*	*C2/c*
a (Å)	31.8764(19)	21.884(6)	20.708(4)
b (Å)	10.3125(6)	17.122(4)	12.429(2)
c (Å)	58.334(3)	23.362(6)	13.446(2)
α (°)	90	90	90
β (°)	104.529(3)	103.18(3)	116.385(2)
γ (°)	90	90	90
V (Å^3)	18562.6(18)	8523(4)	3100.3(10)
Z	8	8	4
D_{calcd} (g/cm^3)	1.439	1.377	1.471
Absorption coefficient, mm^{-1}	0.773	0.580	0.772
F(000)	8,248	3,664	1,412
Crystal size, mm	0.26 x 0.25 x 0.22	0.27 x 0.26 x 0.22	0.23 x 0.23 x 0.18
θ range, deg	2.257 - 28.399	1.49 - 26.37	1.97 - 27.48
Index range *h*, *k*, *l*	-42/42, -13/13, -74/77	-27/26, -18/21, -29/18	-16/26, -16/16, -17/14
Reflections collected	209,919	23,754	9,226
Independent reflections (R_{int})	23,156 (0.0446)	8,702(0.1171)	3,552(0.0362)
Data/restraint/parameters	23,156/565/1281	8,702/0/547	3,552/0/206
Goodness-of-fit on F^2	1.039	0.974	1.013
Final R_1, wR_2 ($I > 2\sigma(I)$)	0.0529, 0.1317	0.0683, 0.1486	0.0380, 0.0891
Largest diff. peak and hole	0.635, -0.594	1.011, -0.402	0.341, -0.237

Table S2 Selected bond lengths [Å] and angles [°] for complexes **1**–**6**.

Parameter	Value	Parameter	Value
1			
Co(1)–O(2)	1.997(3)	Co(1)–O(3)	2.031(3)
Co(1)–N(1)	2.046(4)	Co(1)–N(4)A	2.067(4)
Co(1)–O(4)	2.409(4)		
O(2)–Co(1)–O(3)	100.20(15)	O(2)–Co(1)–N(1)	111.97(15)
O(3)–Co(1)–N(1)	128.83(17)	O(2)–Co(1)–N(4)A	99.24(15)
O(3)–Co(1)–N(4)A	107.83(16)	N(1)–Co(1)–N(4)A	105.03(16)
O(2)–Co(1)–O(4)	158.50(13)	O(3)–Co(1)–O(4)	58.52(14)
N(1)–Co(1)–O(4)	86.41(14)	N(4)A–Co(1)–O(4)	85.90(15)
2			
Co(1)–N(2)	2.099(2)	Co(1)–O(1)A	2.154 (2)
Co(1)–N(2)A	2.099(2)	Co(1)–O(2)A	2.183(2)
Co(1)–O(1)	2.154 (2)	Co(1)–O(2)	2.183(2)
N(2)–Co(1)–N(2)A	93.31(12)	O(1)–Co(1)–O(2)A	102.00(7)
N(2)–Co(1)–O(1)	94.70(8)	O(1)A–Co(1)–O(2A	60.44(7)
N(2)A–Co(1)–O(1)	100.64(8)	N(2)–Co(1)–O(2)	154.66(8)
N(2)–Co(1)–O(1)A	100.64(8)	N(2)A–Co(1)–O(2)	96.03(8)
N(2)A–Co(1)–O(1)A	94.70(8)	O(1)–Co(1)–O(2)	60.44(7)
O(1)–Co(1)–O(1)A	157.61(11)	O(1)A–Co(1)–O(2)	102.00(7)
N(2)–Co(1)–O(2)A	96.03(8)	O(2)A–Co(1)–O(2)	85.40(10)
N(2)A–Co(1)–O(2)A	154.66(8)		
3			
Co(1)–O(1)	2.044(2)	Co(1)–O(3)B	2.135(2)
Co(1)–N(4)A	2.064(2)	Co(1)–O(4)B	2.251(2)
Co(1)–N(1)	2.065(2)	Co(1)–O(2)	2.398(2)
O(1)–Co(1)–N(4)A	102.07(10)	N(1)–Co(1)–O(4)B	166.83(9)
O(1)–Co(1)–N(1)	98.64(10)	O(3)B–Co(1)–O(4)B	59.57(9)
N(4)A–Co(1)–N(1)	99.43(10)	O(1)–Co(1)–O(2)	58.14(9)
O(1)–Co(1)–O(3)B	140.74(10)	N(4)A–Co(1)–O(2)	159.78(9)
N(4)A–Co(1)–O(3)B	102.05(10)	N(1)–Co(1)–O(2)	88.56(9)
N(1)–Co(1)–O(3)B	107.38(9)	O(3)B–Co(1)–O(2)	93.08(9)
O(1)–Co(1)–O(4)B	91.90(9)	O(4)B–Co(1)–O(2)	90.33(10)
N(4)A–Co(1)–O(4)B	85.96(10)		
4			
Co(1)–O(5)	1.955(2)	Co(2)–O(8)	1.985 (2)
Co(1)–O(1)	1.960(2)	Co(2)–O(10)	1.997(3)
Co(1)–N(12)A	2.050(2)	Co(2)–N(7)	2.071(2)
Co(1)–N(4)	2.054(2)	Co(2)–N(5)	2.073(2)

Co(3)–O(11)	2.011(2)	Co(3)–N(1)C	2.153(2)
Co(3)–N(9)	2.081(2)	Co(3)–O(1W)	2.228(3)
Co(3)–O(3)B	2.085(2)	Co(3)–O(4)B	2.258(2)
O(5)–Co(1)–O(1)	128.35(10)	O(11)–Co(3)–O(3)B	104.26(9)
O(5)–Co(1)–N(12)A	114.95(9)	N(9)–Co(3)–O(3)B	145.17(8)
O(1)–Co(1)–N(12)A	100.64(8)	O(11)–Co(3)–N(1)C	89.83(8)
O(5)–Co(1)–N(4)	102.24(8)	N(9)–Co(3)–N(1)C	94.00(9)
O(1)–Co(1)–N(4)	106.69(8)	O(3)B–Co(3)–N(1)C	102.93(9)
N(12)A–Co(1)–N(4)	100.61(9)	O(11)–Co(3)–O(1W)	85.96(11)
O(8)–Co(2)–O(10)	140.70(12)	N(9)–Co(3)–O(1W)	84.90(12)
O(8)–Co(2)–N(7)	98.66(9)	O(3)B–Co(3)–O(1W)	80.45(12)
N(7)–Co(2)–N(5)	98.16(9)	N(1)C–Co(3)–O(1W)	175.16(10)
O(10)–Co(2)–N(7)	106.52(11)	O(11)–Co(3)–O(4)B	163.21(8)
O(8)–Co(2)–N(5)	103.84(9)	N(9)–Co(3)–O(4)B	88.39(7)
O(11)–Co(3)–N(9)	106.02(9)	O(3)B–Co(3)–O(4)B	59.53(7)
O(10)–Co(2)–N(5)	101.89(9)	N(1)C–Co(3)–O(4)B	97.86(8)
O(1W)–Co(3)–O(4)B	86.83(11)		

5

Co(1)–O(6)	2.075(4)	Co(1)–N(3)A	2.108(4)
Co(1)–O(1)B	2.138(3)	Co(1)–N(1)	2.156(4)
Co(1)–N(5)	2.162(4)	Co(1)–O(2)B	2.285(4)
O(6)–Co(1)–N(3)A	99.62(15)	O(6)–Co(1)–O(1)B	94.21(14)
N(3)A–Co(1)–O(1)B	165.59(16)	O(6)–Co(1)–N(1)	93.95(16)
N(3)A–Co(1)–N(1)	84.78(15)	O(1)B–Co(1)–N(1)	90.27(15)
O(6)–Co(1)–N(5)	92.30(15)	N(3)A–Co(1)–N(5)	88.61(15)
O(1)B–Co(1)–N(5)	94.90(15)	N(1)–Co(1)–N(5)	171.58(16)
O(6)–Co(1)–O(2)B	152.82(14)	N(3)A–Co(1)–O(2)B	107.27(15)
O(1)B–Co(1)–O(2)B	59.34(14)	N(1)–Co(1)–O(2)B	92.41(15)
N(5)–Co(1)–O(2)B	84.56(14)		

6

Co(1)–N(1)A	2.076(2)	Co(1)–N(1)	2.076(2)
Co(1)–O(2)	2.163(2)	Co(1)–O(2)A	2.163(2)
Co(1)–O(1)A	2.173(2)	Co(1)–O(1)	2.173(2)
N(1)A–Co(1)–N(1)	95.90(11)	N(1)A–Co(1)–O(2)	99.27(7)
N(1)–Co(1)–O(2)	93.58(7)	N(1)A–Co(1)–O(2)A	93.58(7)
N(1)–Co(1)–O(2)A	99.27(7)	O(2)–Co(1)–O(2)A	160.79(9)
N(1)A–Co(1)–O(1)A	153.04(7)	N(1)–Co(1)–O(1)A	94.61(7)
O(2)–Co(1)–O(1)A	104.78(6)	O(2)A–Co(1)–O(1)A	60.19(6)
N(1)A–Co(1)–O(1)	94.61(7)	N(1)–Co(1)–O(1)	153.04(7)
O(2)–Co(1)–O(1)	60.19(6)	O(2)A–Co(1)–O(1)	104.78(6)

O(1)A–Co(1)–O(1)	87.01(10)

Symmetry codes for **1**: A: *x*, *y*+1, *z*; for **2**: A: -*x*+1, *y*, *z*+3/2; for **3**: A: *x*+1, -*y*+1/2, *z*+1/2; B: -*x*+1, *y*-1/2, -*z*+3/2; for **4**: A: -*x*+3/2, *y*, -*z*+1; B: *x*+1, -*y*+3/2, *z*-1/2; C: -*x*+2, -*y*, -*z*+1; for **5**: A: -*x*, *y*, -*z*+1/2; B: -*x*+1/2, *y*-1/2, -*z*+1; for **6**: A: –*x*+1, *y*, –*z* +1/2; B: -*x*+3/2, -*y*+3/2, -*z*+1;

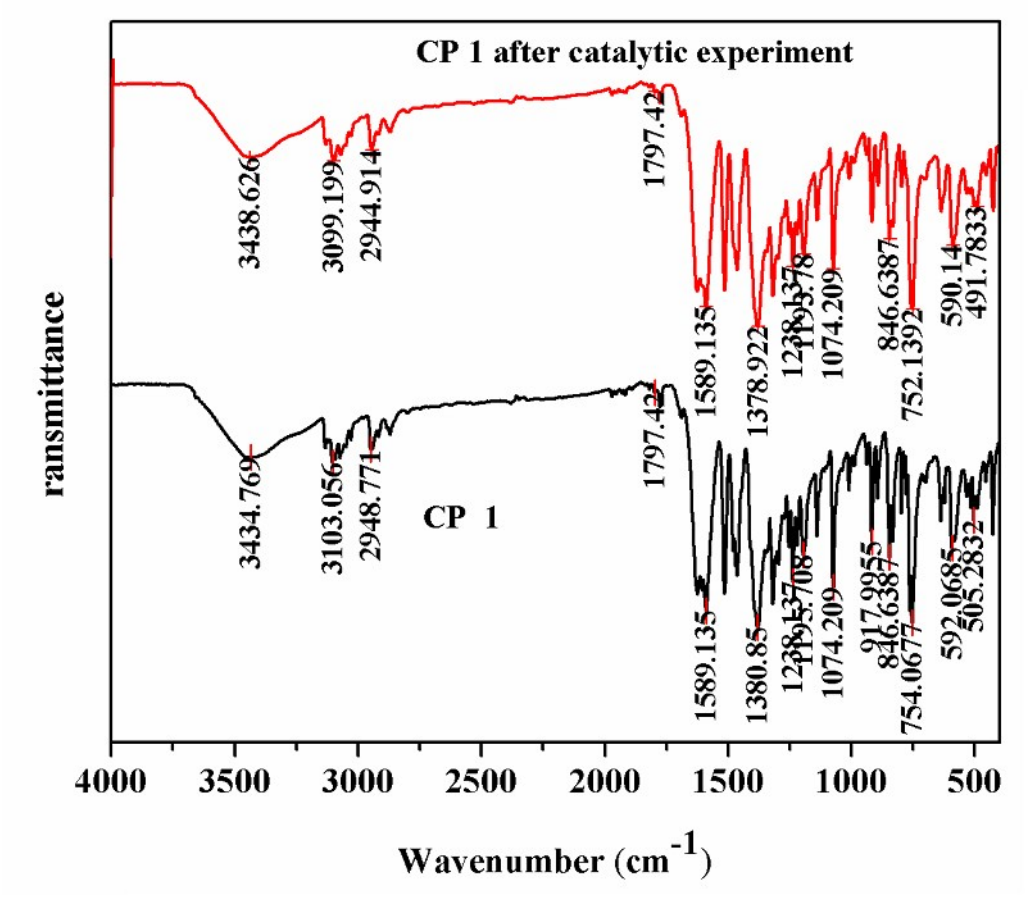
CP 1 after catalytic experiment
3438.626
3099.199
2944.914
1797.42
1589.135
1378.922
1074.209
846.6387
752.1392
590.14
491.7833
CP 1
3434.769
3103.056
2948.771
1797.42
1589.135
1380.85
1074.209
754.0677
592.0685
505.2832
ransmittance
4000
3500
3000
2500
2000
1500
1000
500
Wavenumber (cm-1)

(a)

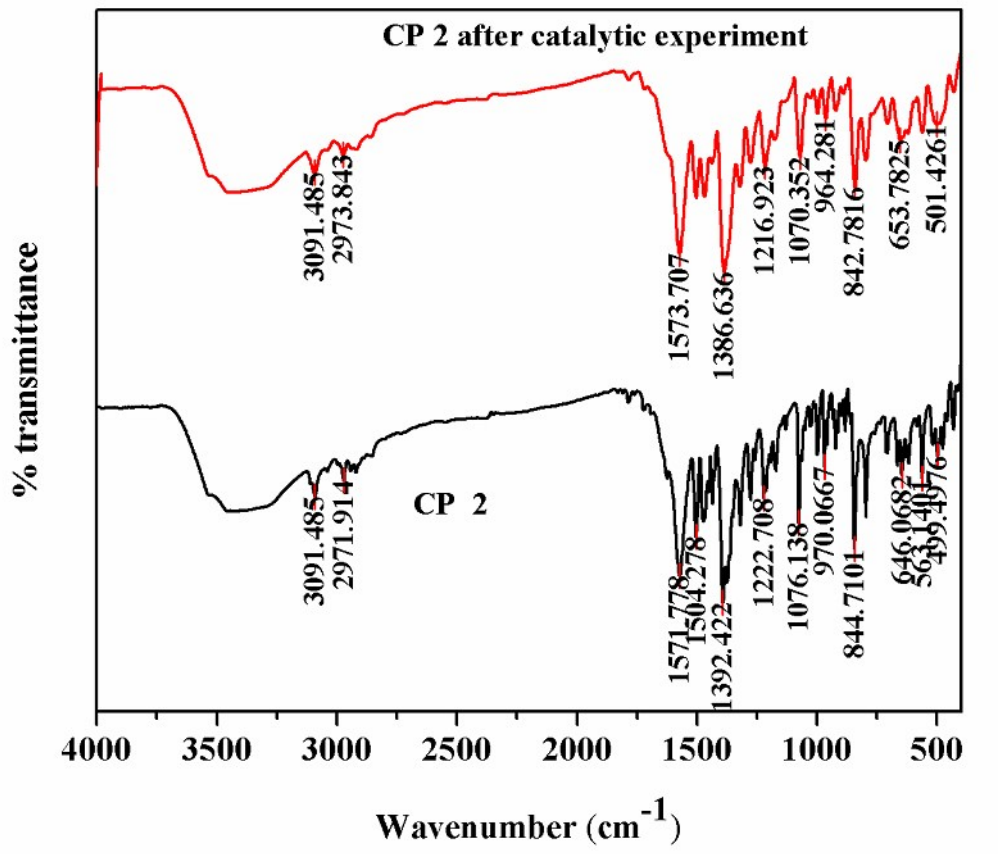
CP 2 after catalytic experiment
3091.485
2973.843
1573.707
1386.636
1216.923
1070.352
964.281
842.7816
653.7825
501.4261
CP 2
3091.485
2971.914
1571.778
1504.278
1392.422
1222.708
1076.138
970.0667
844.7101
% transmittance
4000
3500
3000
2500
2000
1500
1000
500
Wavenumber (cm-1)

(b)

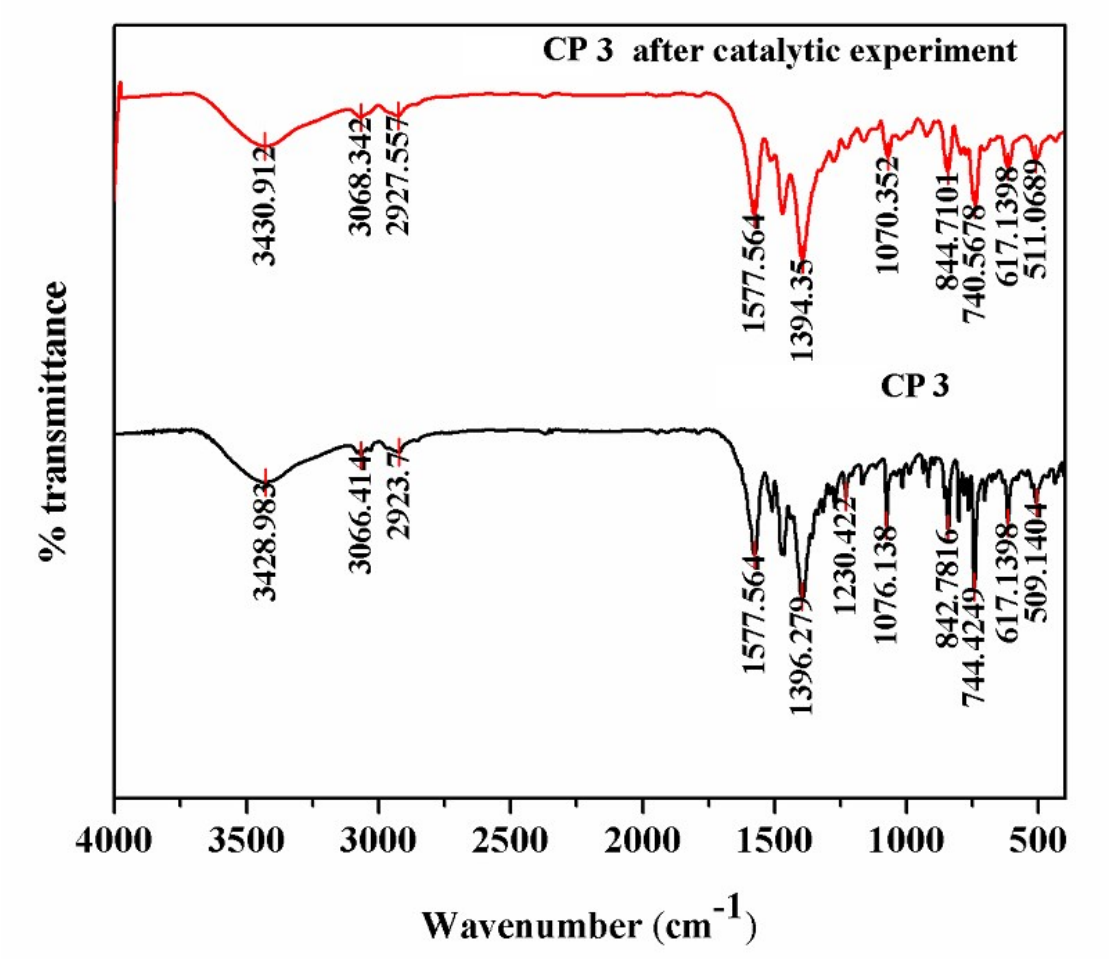
CP 3 after catalytic experiment
3430.912
3068.342
2927.557
1577.564
1394.35
1070.352
844.7101
740.5678
617.1398
511.0689
CP 3
3428.983
3066.414
2923.7
1577.564
1396.279
1230.422
1076.138
842.7816
744.4249
617.1398
509.1404
% transmittance
4000
3500
3000
2500
2000
1500
1000
500
Wavenumber (cm-1)

(c)

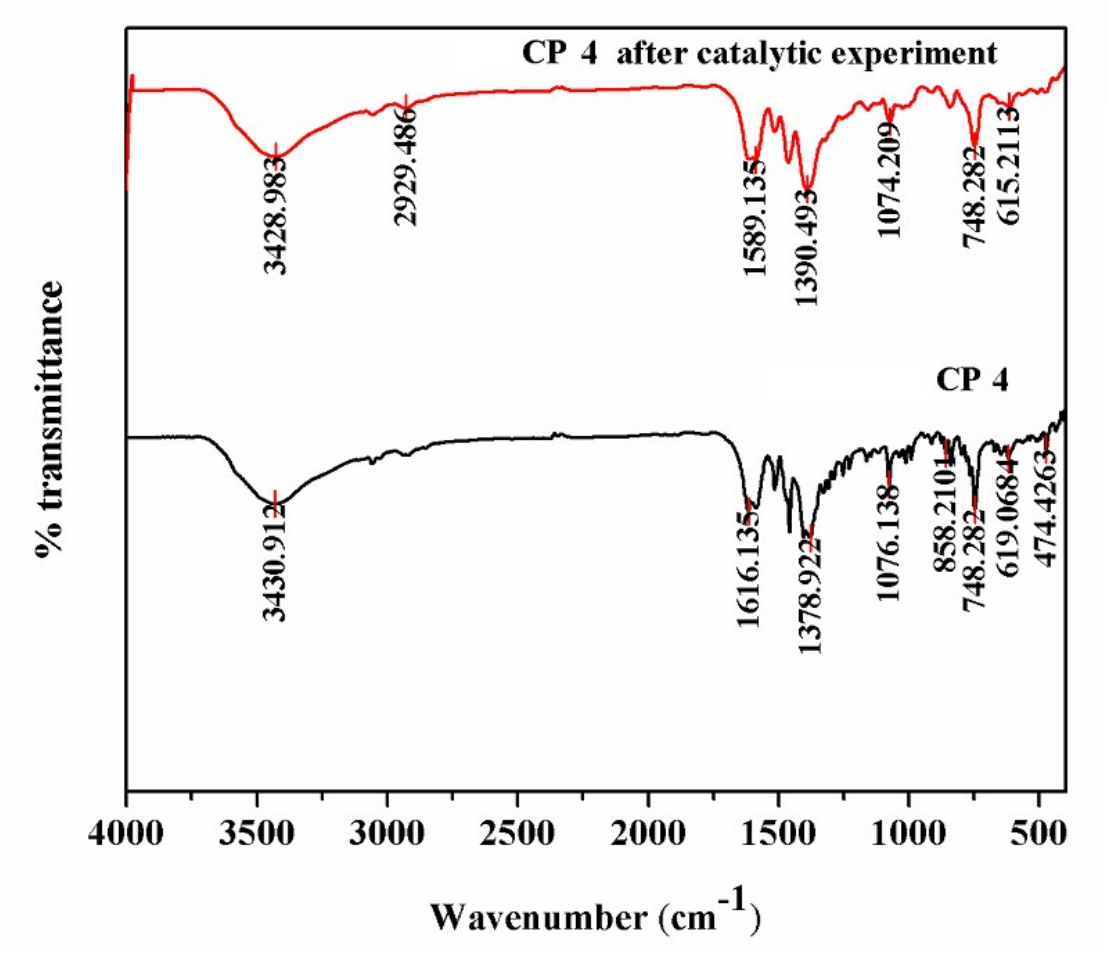
CP 4 after catalytic experiment
3428.983
2929.486
1589.135
1390.493
1074.209
748.282
615.2113
CP 4
3430.912
1616.135
1378.922
1076.138
858.2101
748.282
619.0684
474.4263
% transmittance
4000
3500
3000
2500
2000
1500
1000
500
Wavenumber (cm-1)

(d)

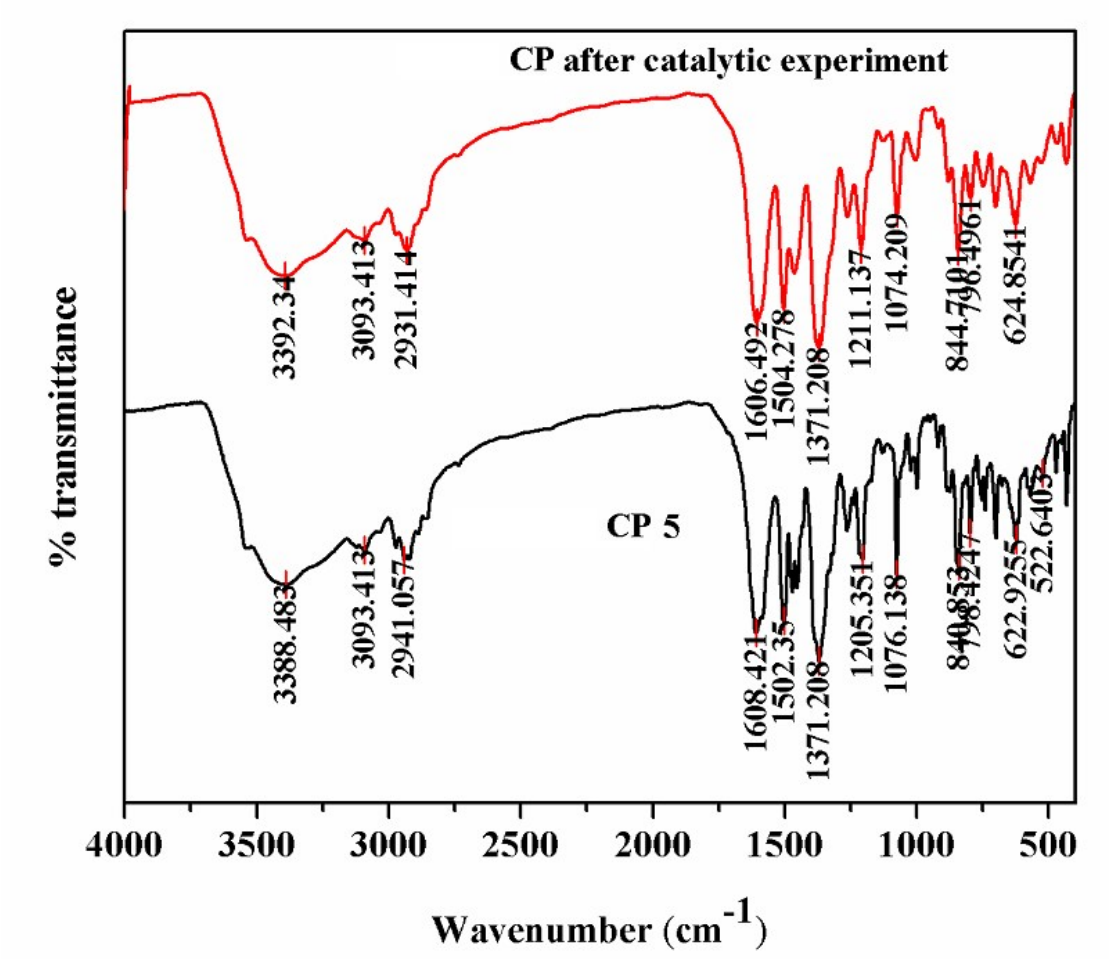
CP after catalytic experiment
CP 5
% transmittance
Wavenumber (cm-1)
4000
3500
3000
2500
2000
1500
1000
500
3392.34
3093.413
2931.414
1606.492
1504.278
1371.208
1211.137
1074.209
844.7101
798.4961
624.8541
3388.483
3093.413
2941.057
1608.421
1502.35
1371.208
1205.351
1076.138
622.9255
522.6403

(e)

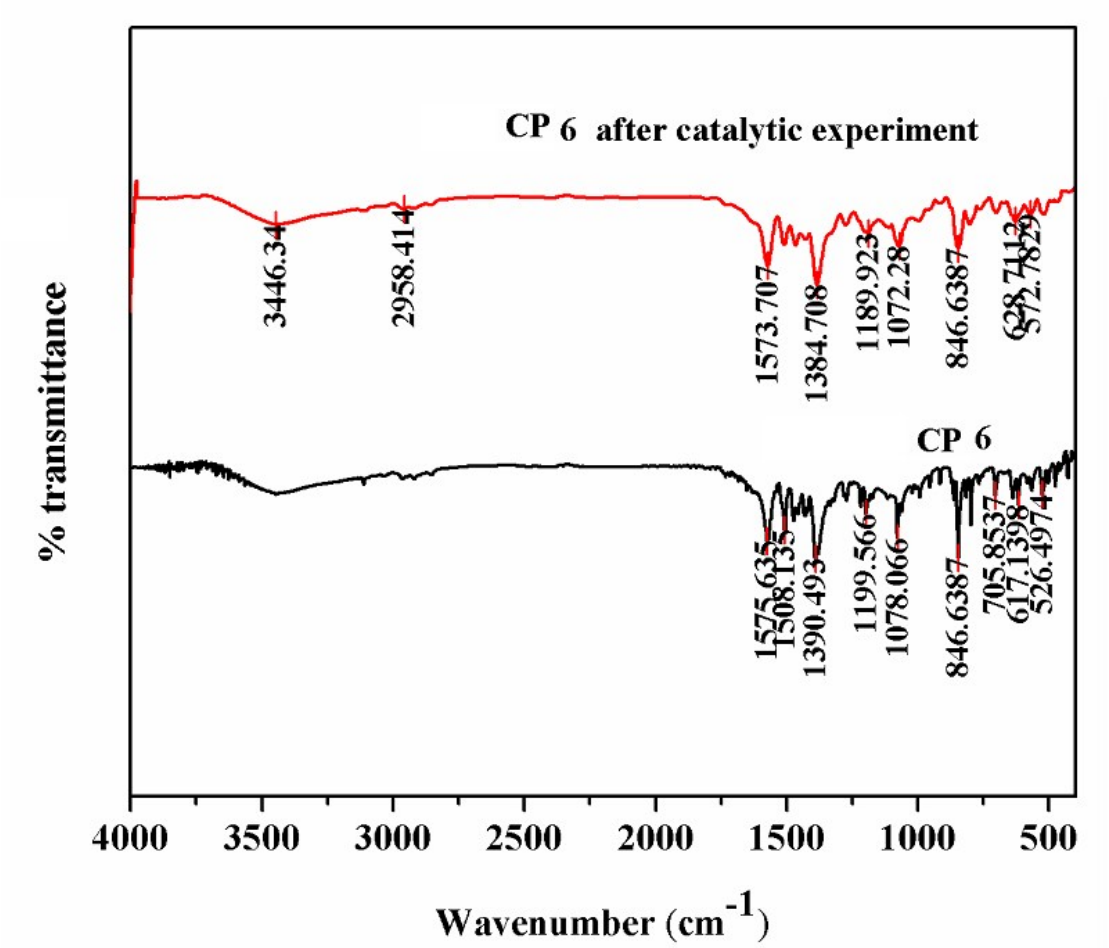

(f)

Fig. S1 The IR spectra of the CPs **1**–**6** (black lines); The IR spectra of the powder of the CPs **1**–**6** after catalytic experiments (red lines).

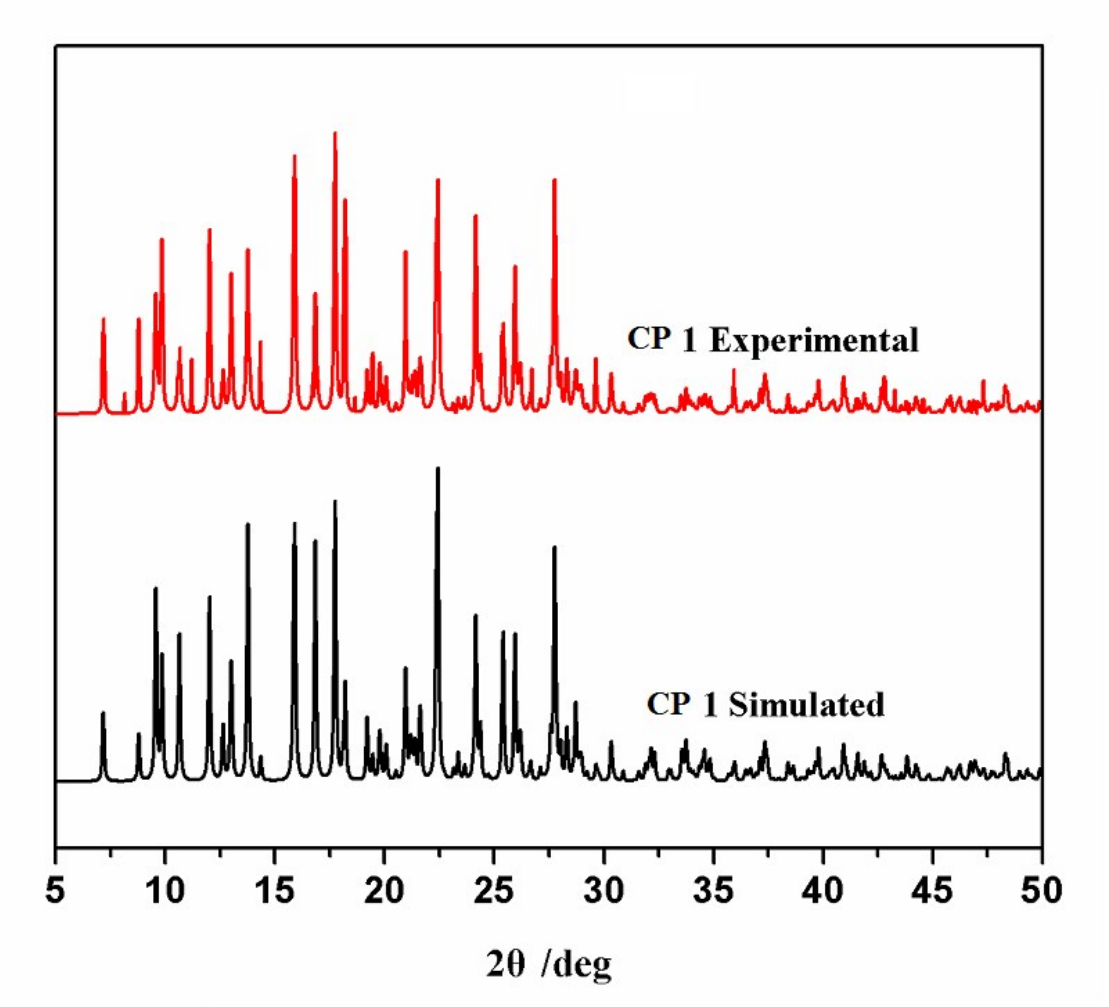

(a)

Fig. S2a The simulated from single-crystal data and obtained from the experiments X-ray powder diffraction patterns of CP **1**.

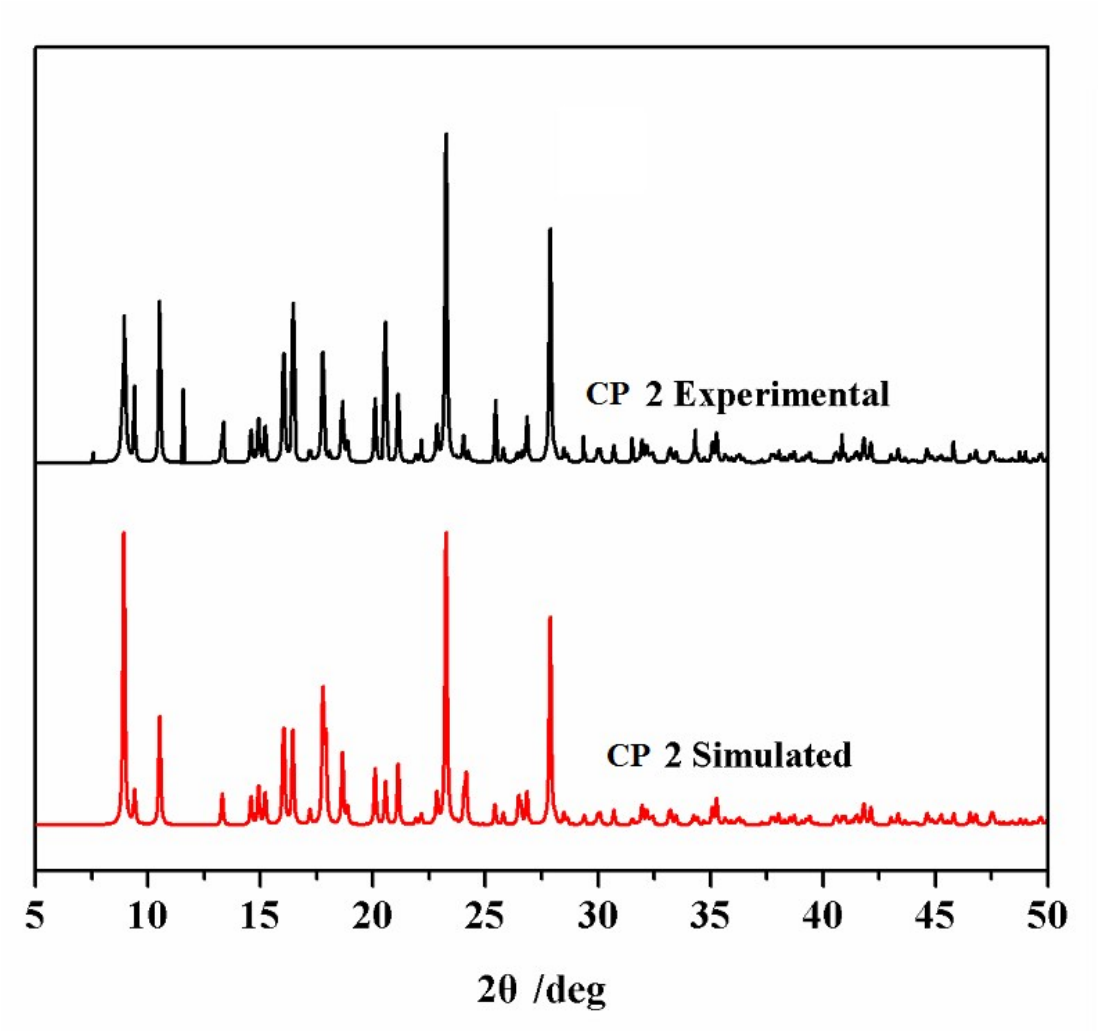

(b)

Fig. S2b The simulated from single-crystal data and obtained from the experiments X-ray powder diffraction patterns of CP **2**.

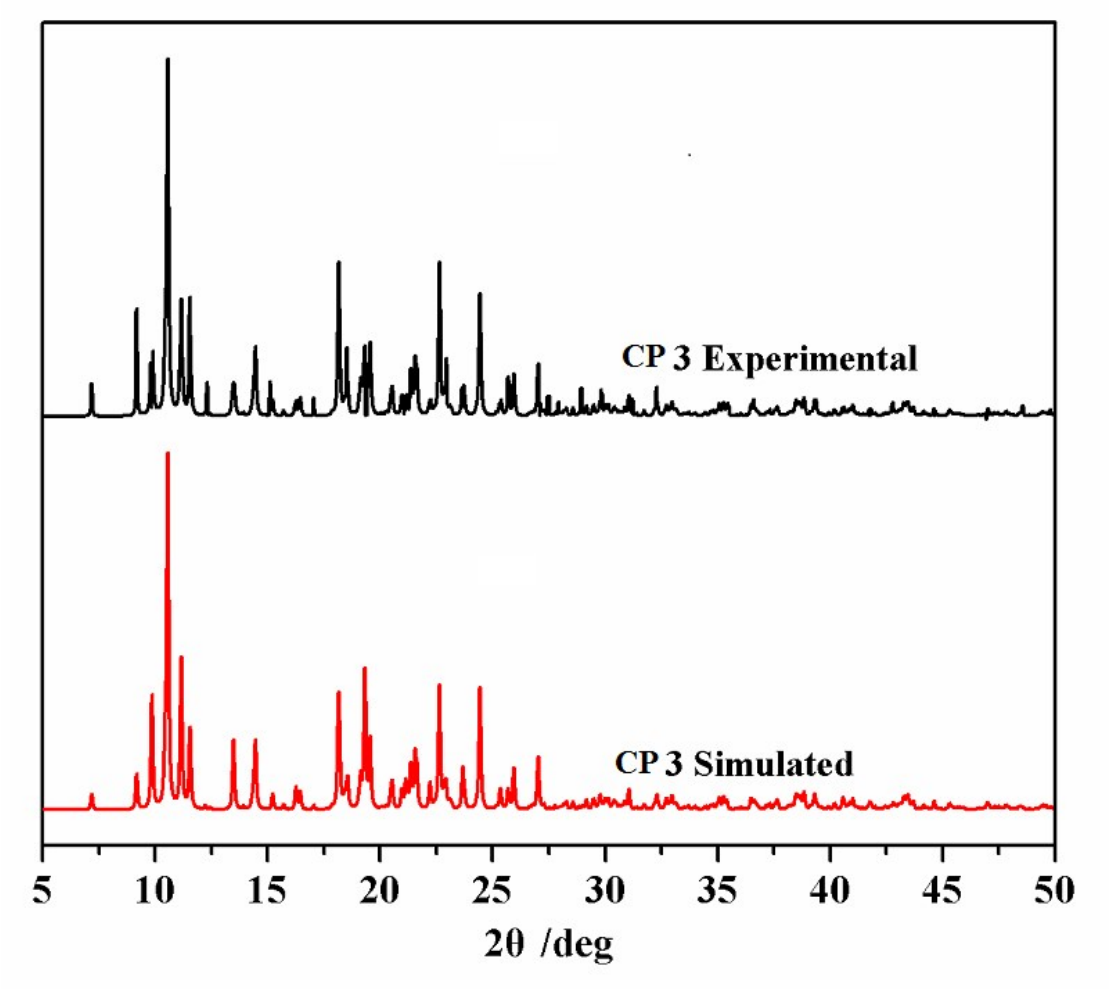

(c)

Fig. S2c The simulated from single-crystal data and obtained from the experiments X-ray powder diffraction patterns of CP **3**.

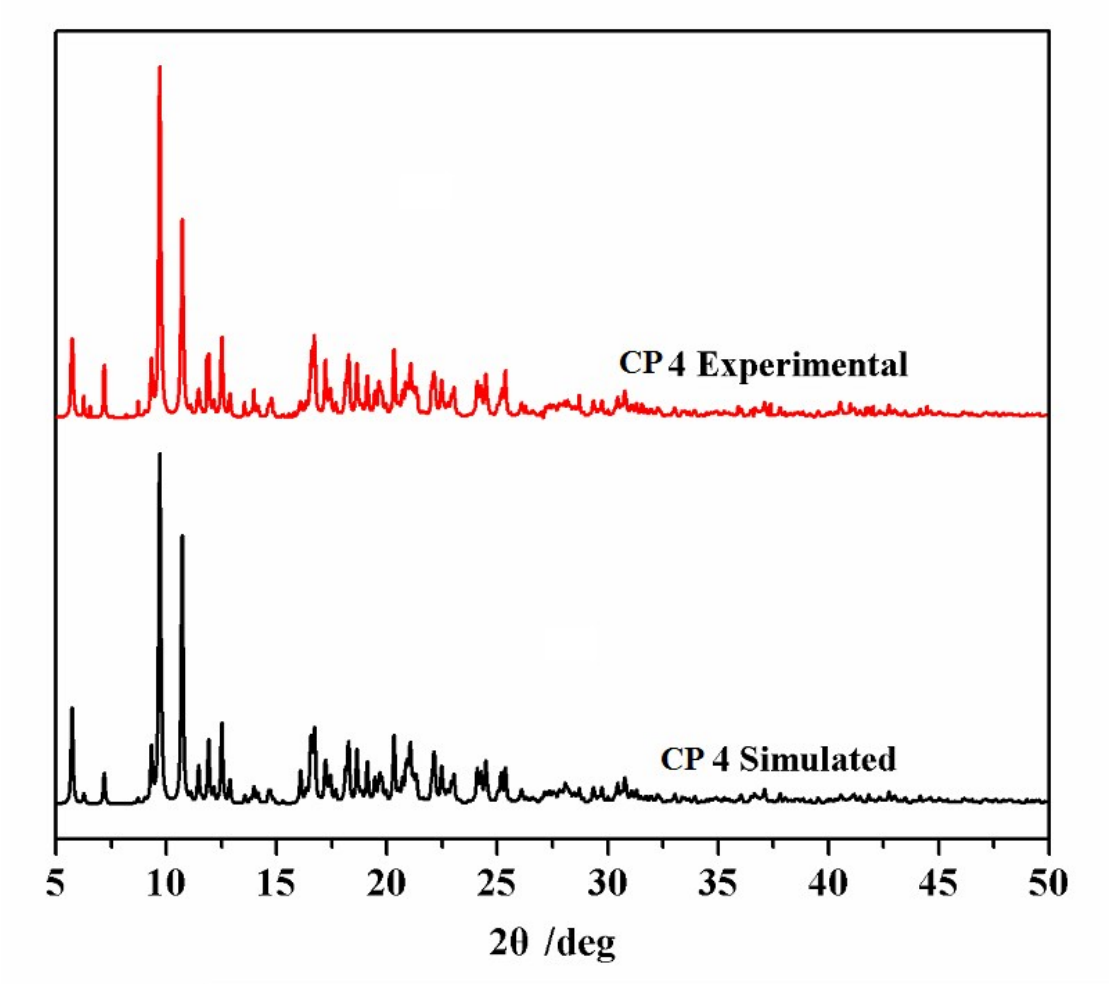

(d)

Fig. S2d The simulated from single-crystal data and obtained from the experiments X-ray powder diffraction patterns of CP **4**.

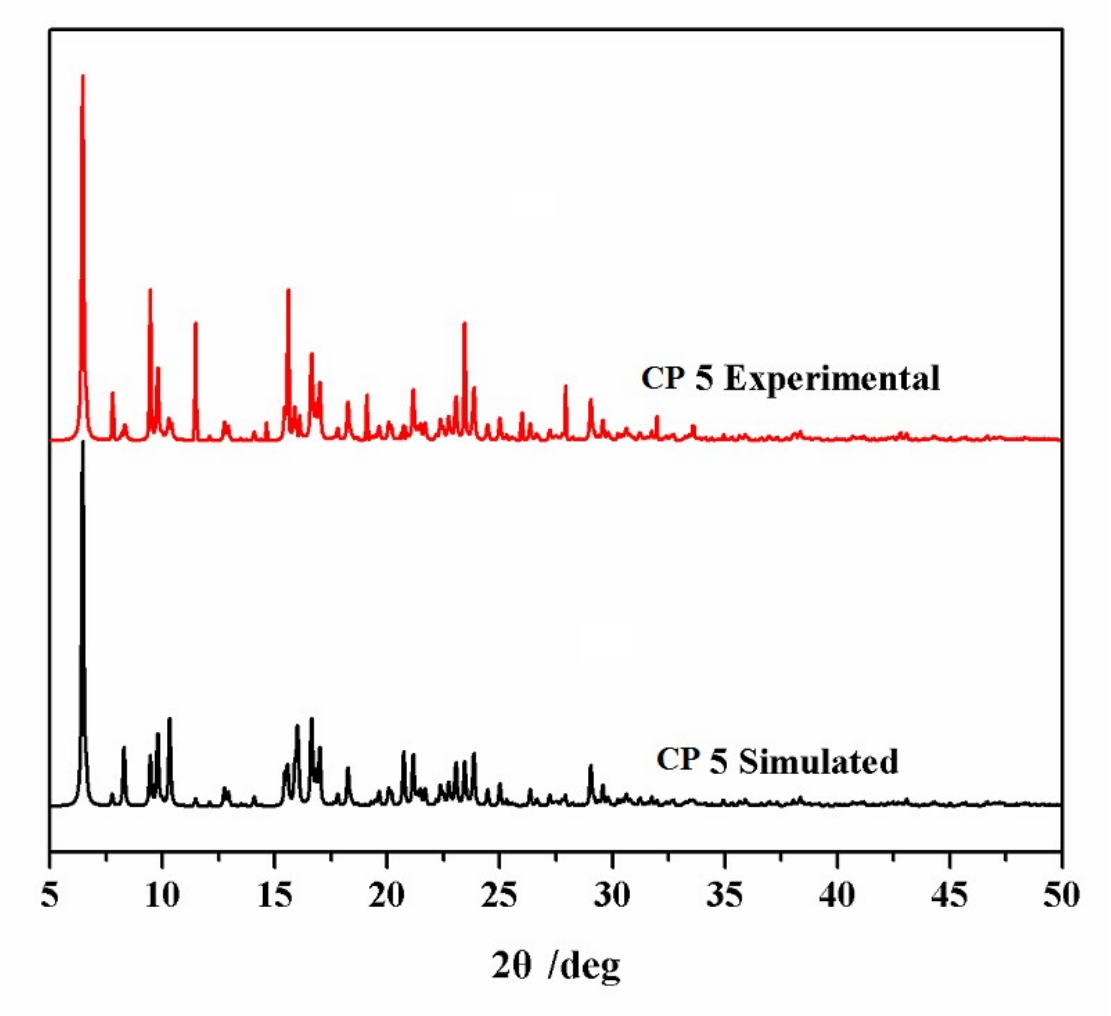

(e)

Fig. S2e The simulated from single-crystal data and obtained from the experiments X-ray powder diffraction patterns of CP **5**.

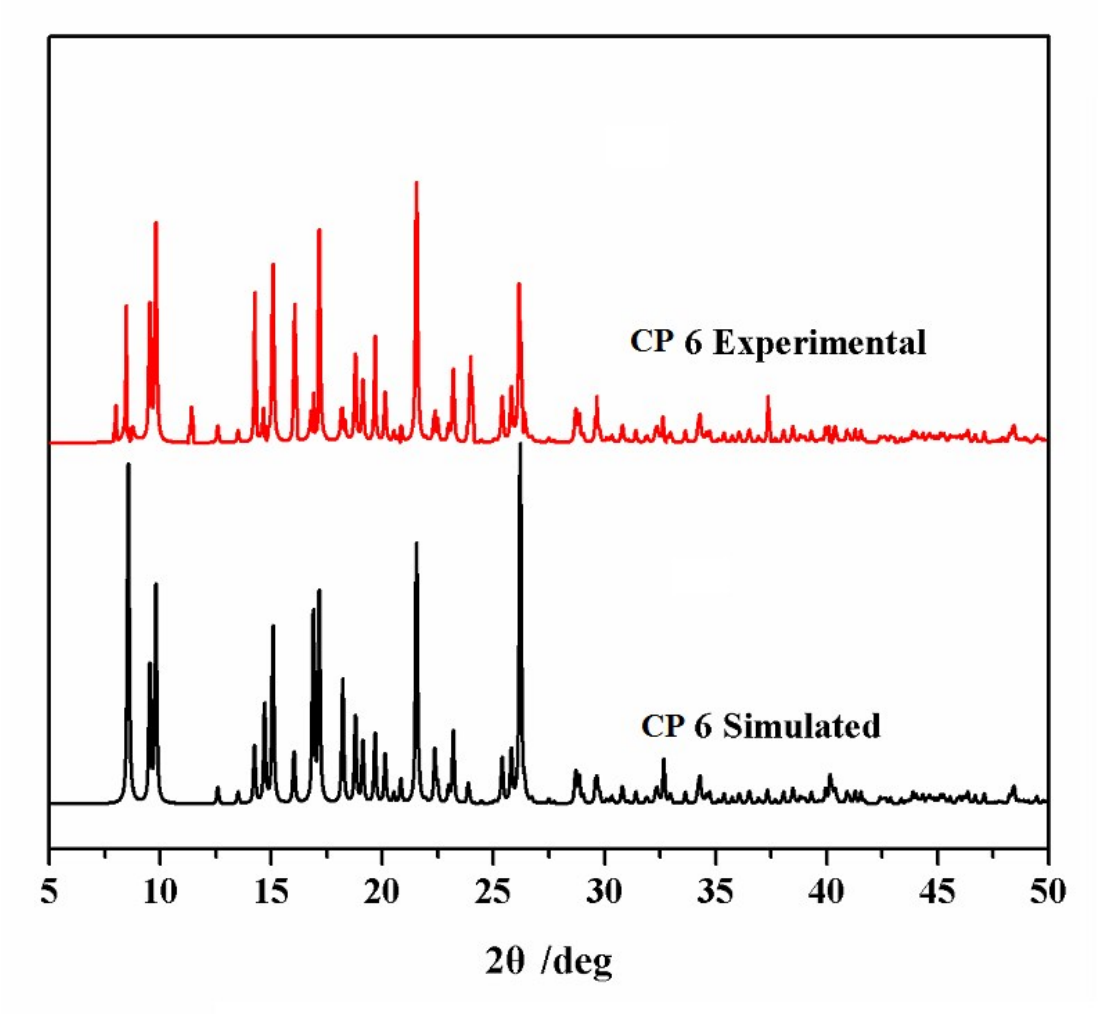

(f)

Fig. S2f The simulated from single-crystal data and obtained from the experiments X-ray powder diffraction patterns of CP **6.**

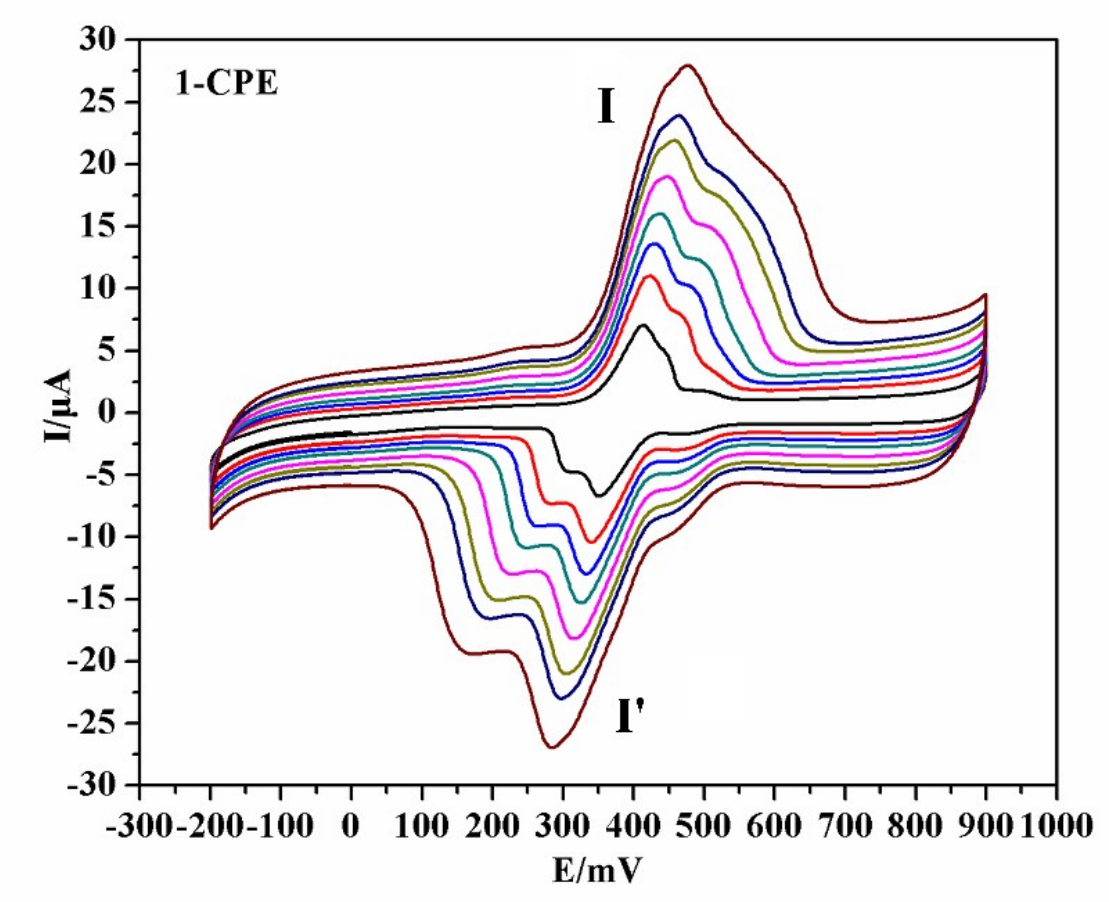

(a)

Fig. **S3a** Cyclic voltammograms of **1**-CPE in 1 M H_2SO_4 solution at various scan rates (from inner to outer: 20, 60, 100, 120, 140, 160, 180 mV s^{-1}).

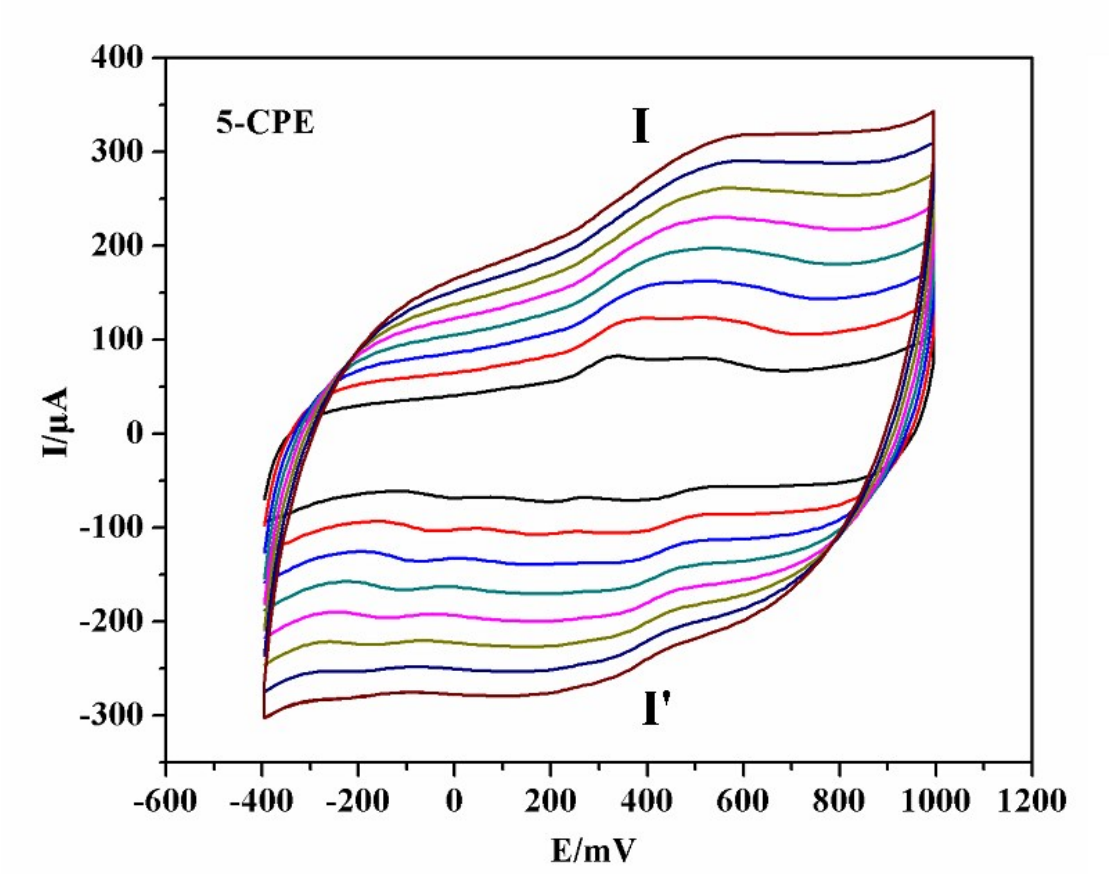

(b)

Fig. **S3b** Cyclic voltammograms of **5**-CPE in 1 M H_2SO_4 solution at various scan rates (from inner to outer: 20, 60, 100, 120, 140, 160, 180 mV s^{-1}).

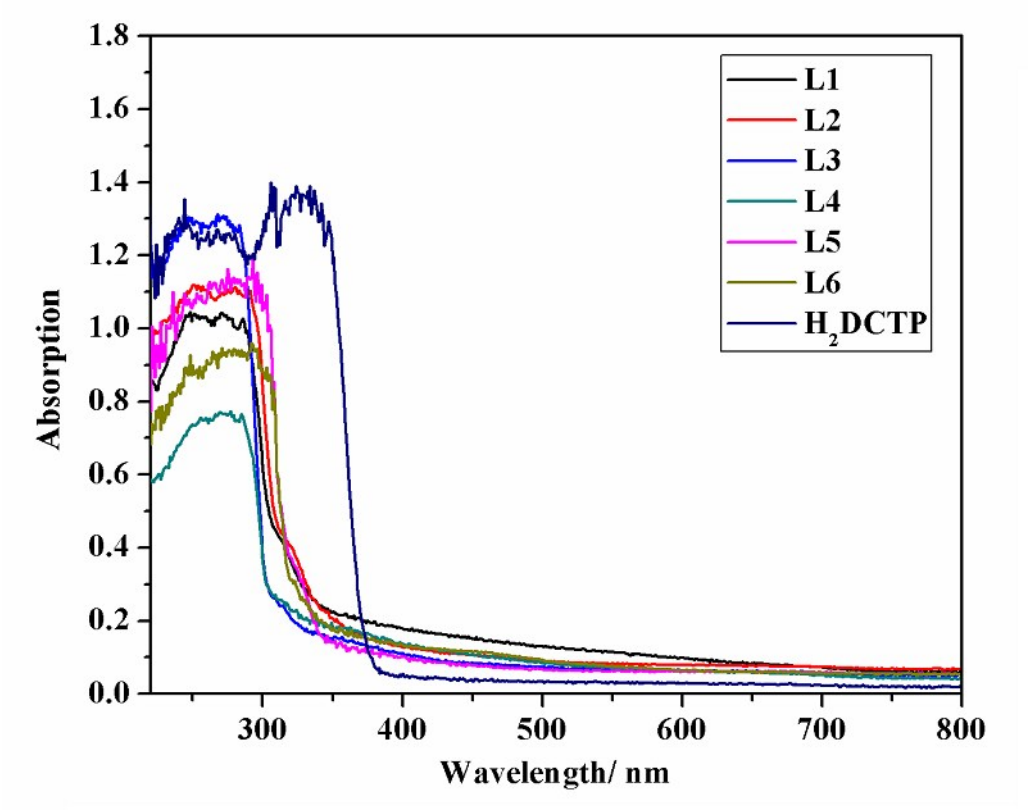
Absorption
Wavelength/ nm
L1
L2
L3
L4
L5
L6
H2DCTP

(a)

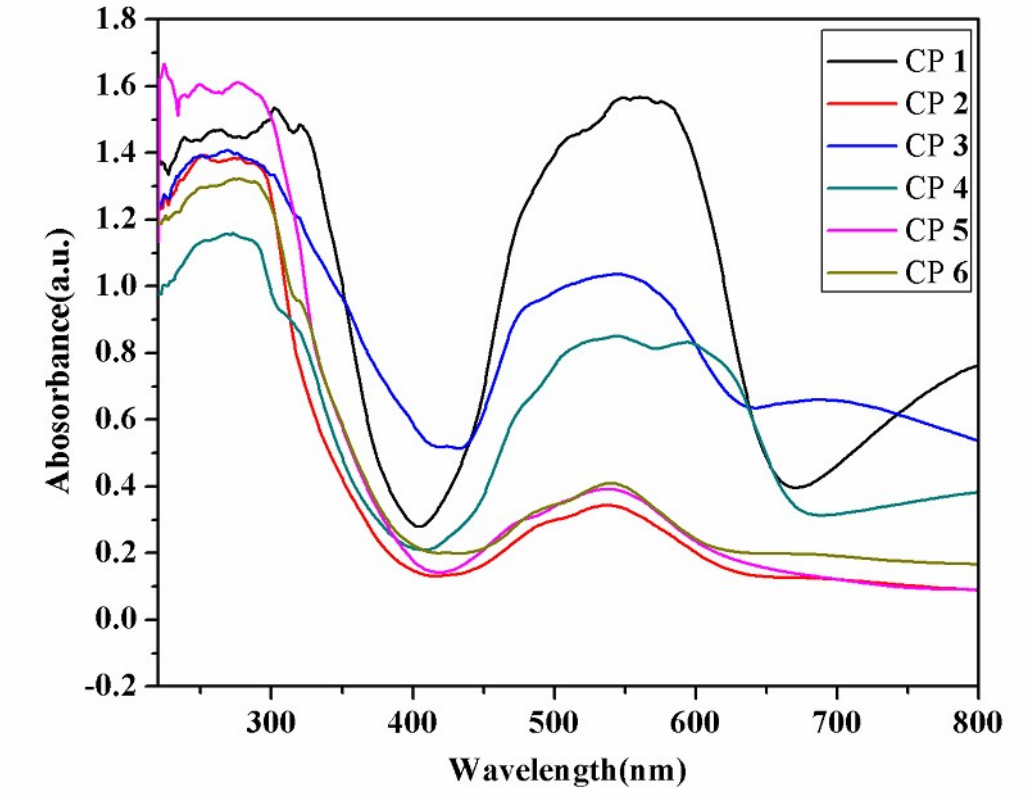
Abosorbance(a.u.)
Wavelength(nm)
CP 1
CP 2
CP 3
CP 4
CP 5
CP 6

(b)

Fig. **S4** UV−vis absorption spectra at room temperature and main absorption bands for the N-donor ligands, H_2DCTP ligand, and CPs **1**–**6**.

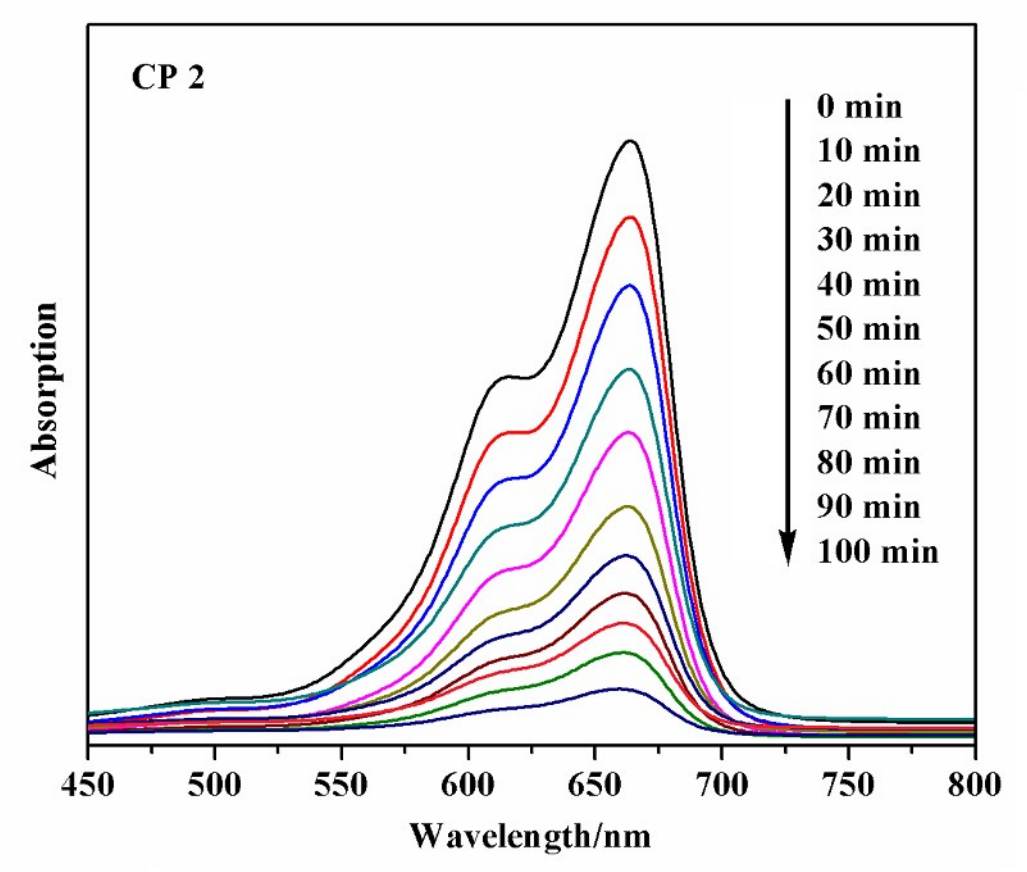

(a)

Fig. **S5a** Absorption spectra of the MB solution during the decomposition reaction under UV irradiation with the presence of CP **2**.

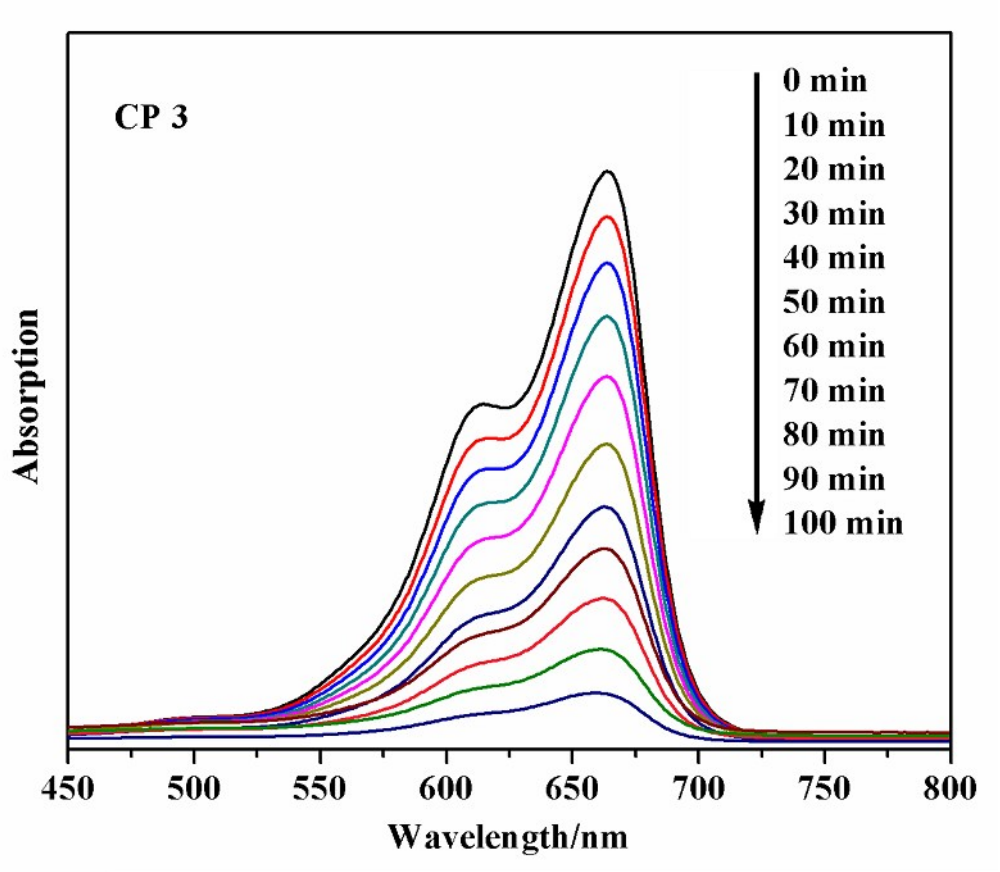

(b)

Fig. **S5b** Absorption spectra of the MB solution during the decomposition reaction under UV irradiation with the presence of CP **3**.

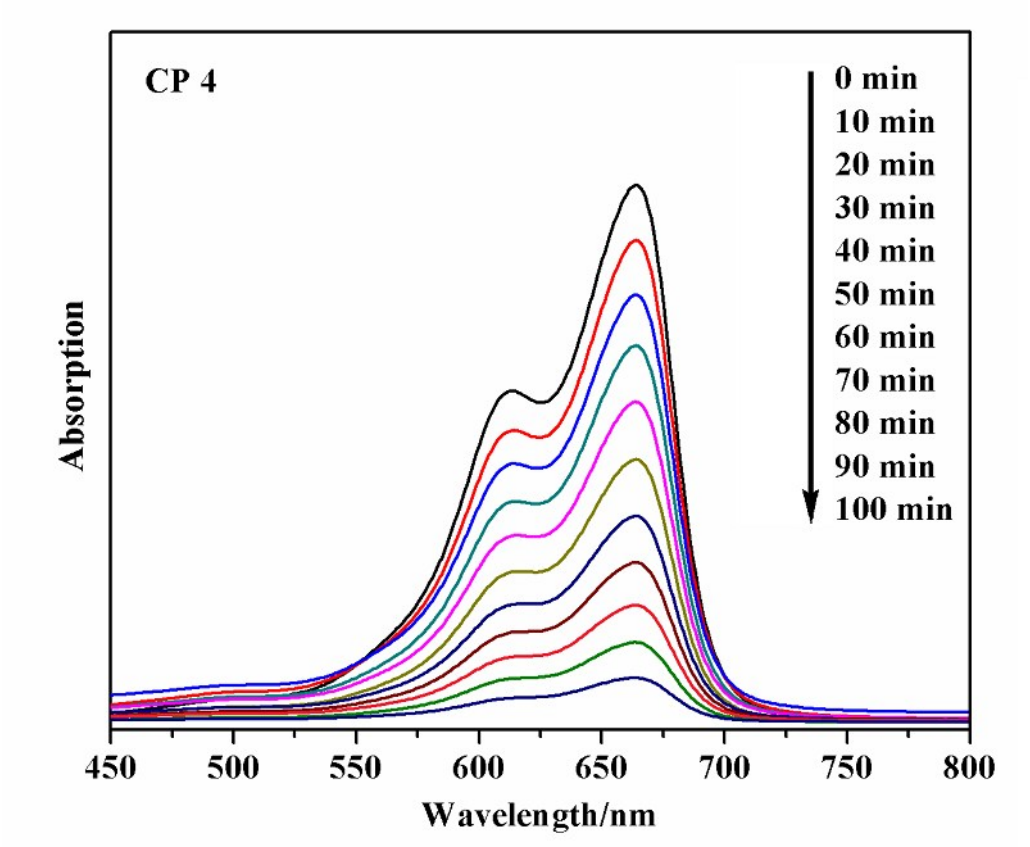

(c)

Fig. **S5c** Absorption spectra of the MB solution during the decomposition reaction under UV irradiation with the presence of CP **4**.

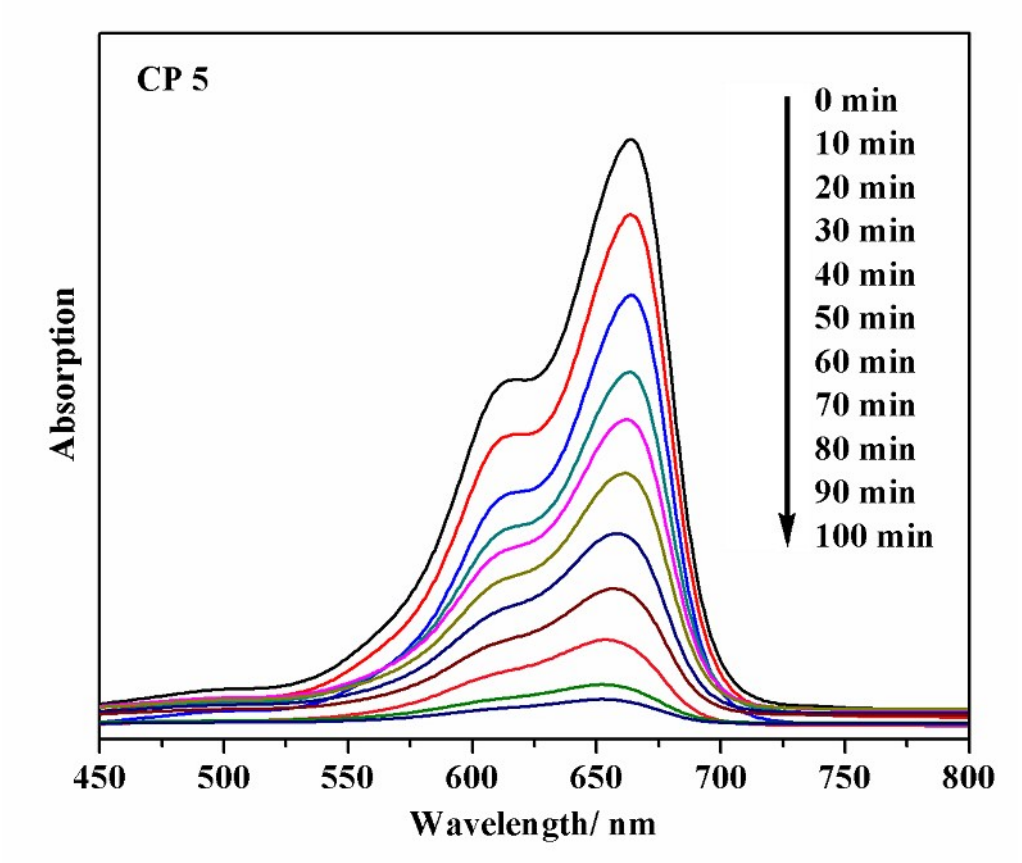

(d)

Fig. **S5d** Absorption spectra of the MB solution during the decomposition reaction under UV irradiation with the presence of CP **5**.

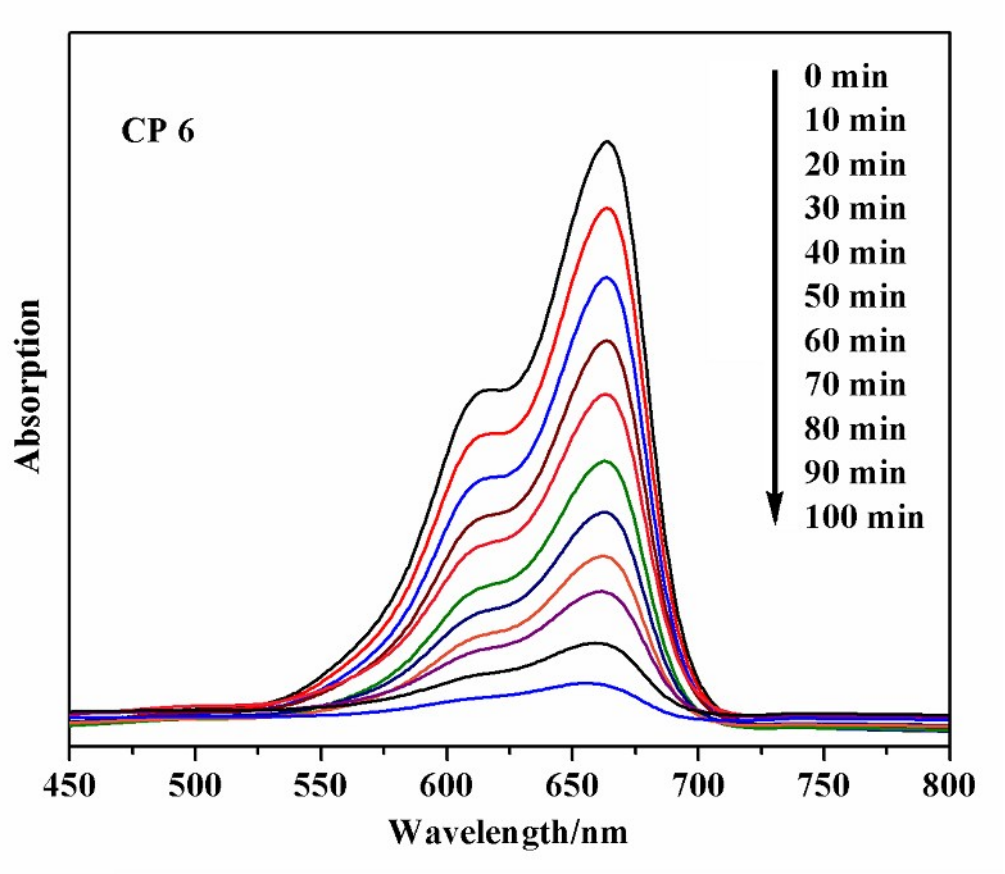

(e)

Fig. **S5e** Absorption spectra of the MB solution during the decomposition reaction under UV irradiation with the presence of CP **6**.

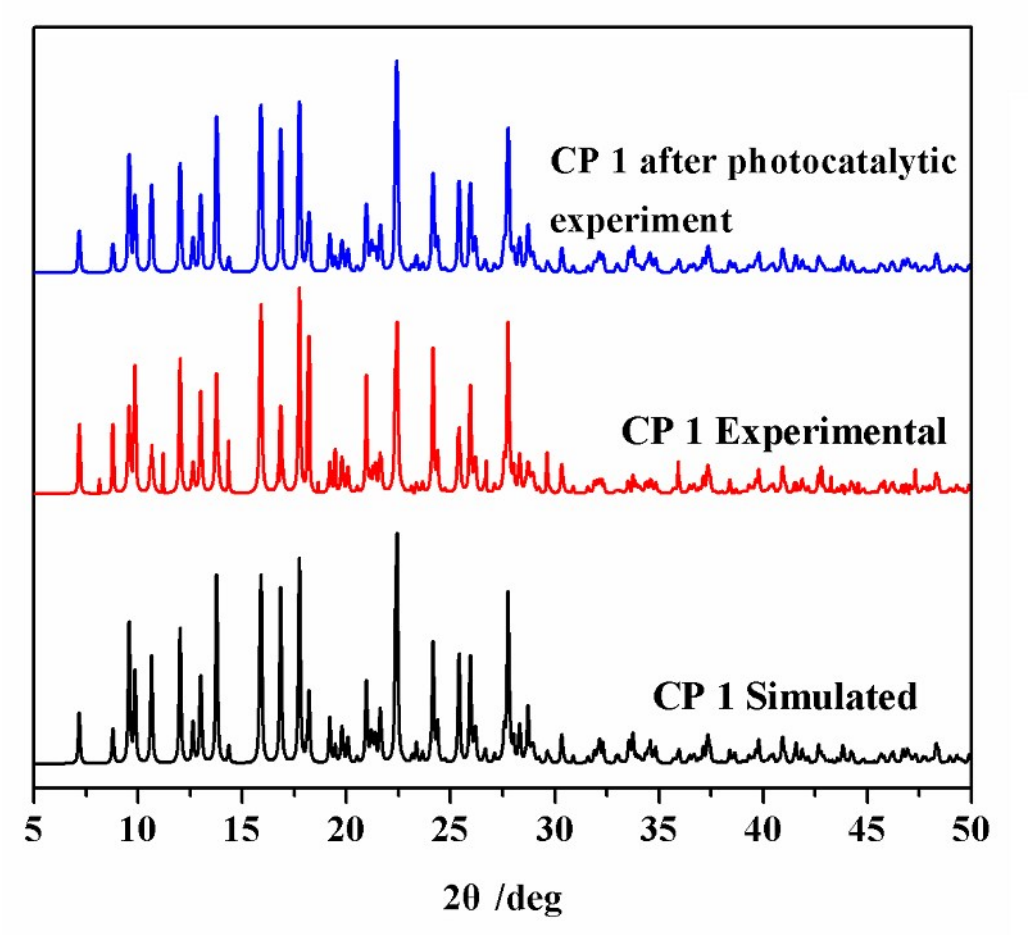
CP 1 after photocatalytic experiment
CP 1 Experimental
CP 1 Simulated
5
10
15
20
25
30
35
40
45
50
2θ /deg

(a)

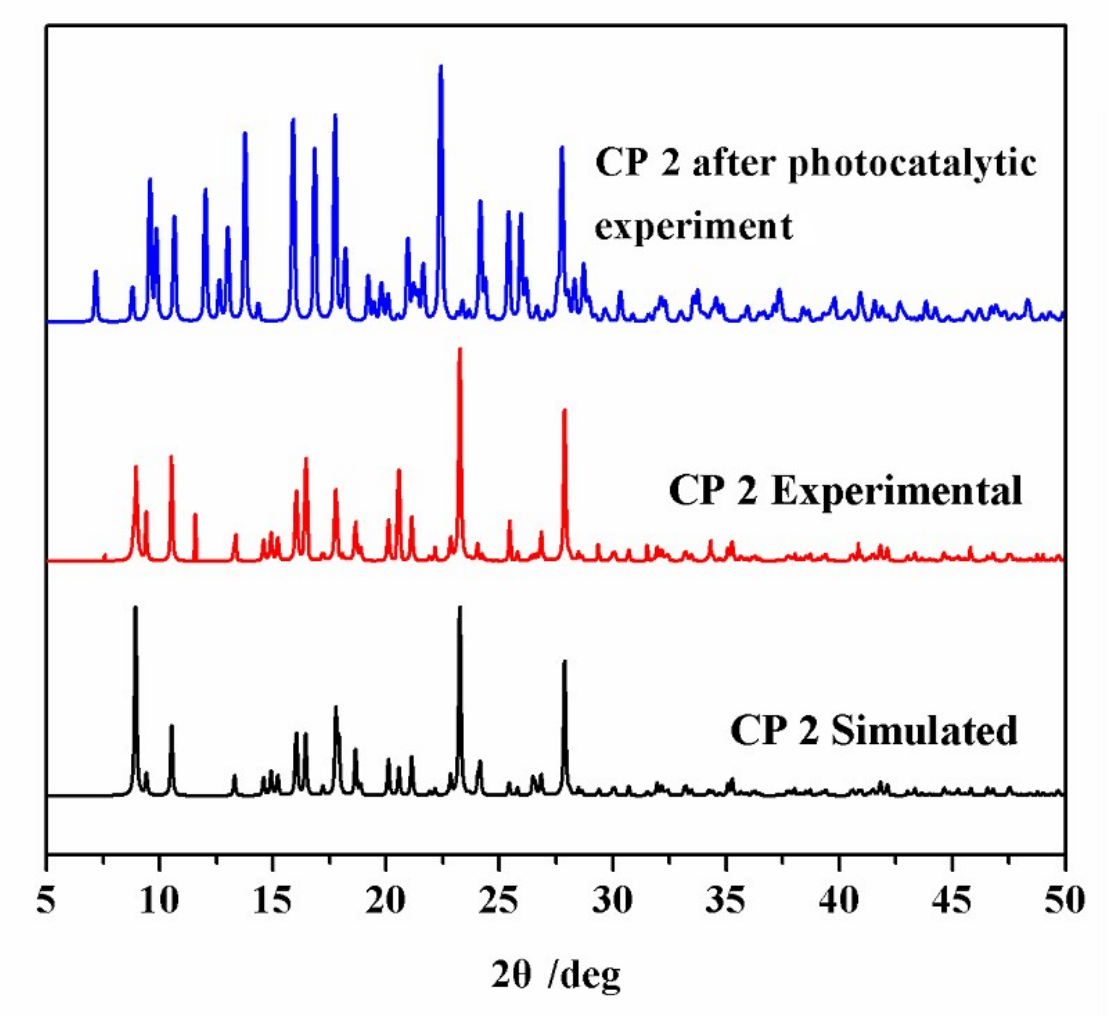
CP 2 after photocatalytic experiment
CP 2 Experimental
CP 2 Simulated
5
10
15
20
25
30
35
40
45
50
2θ /deg

(b)

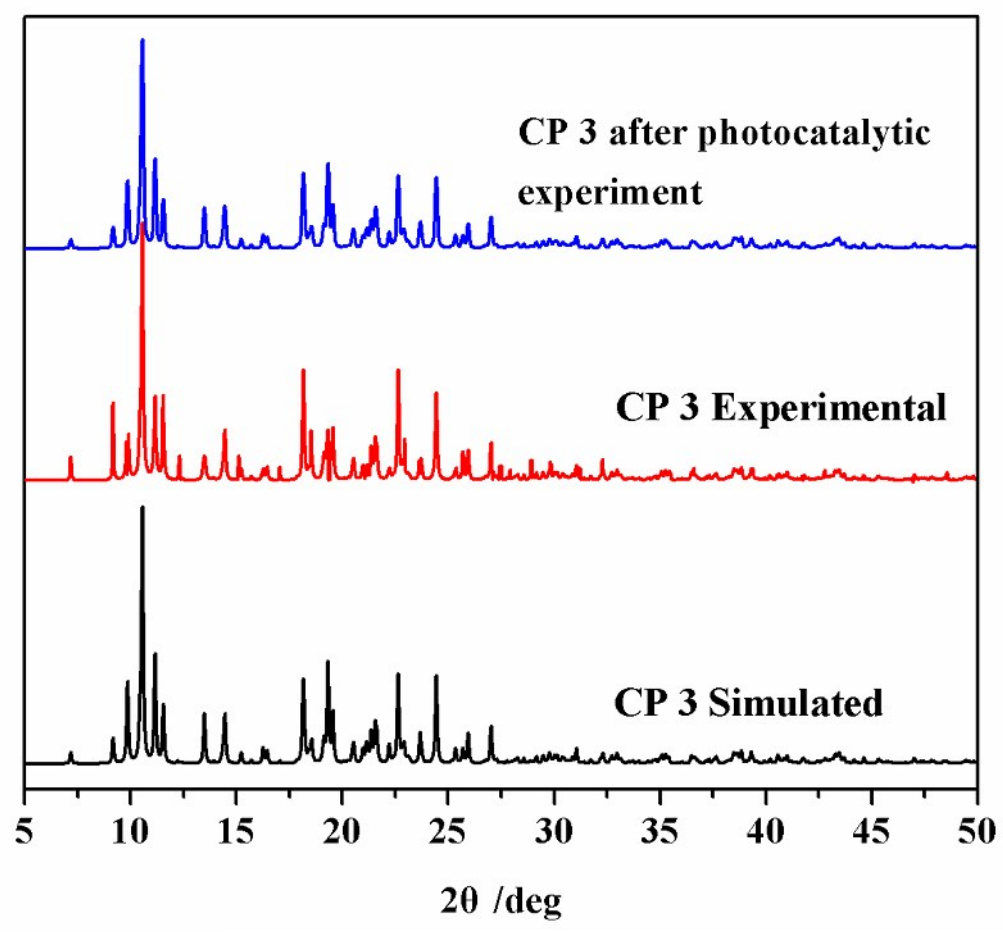
CP 3 after photocatalytic experiment
CP 3 Experimental
CP 3 Simulated
5
10
15
20
25
30
35
40
45
50
2θ /deg

(c)

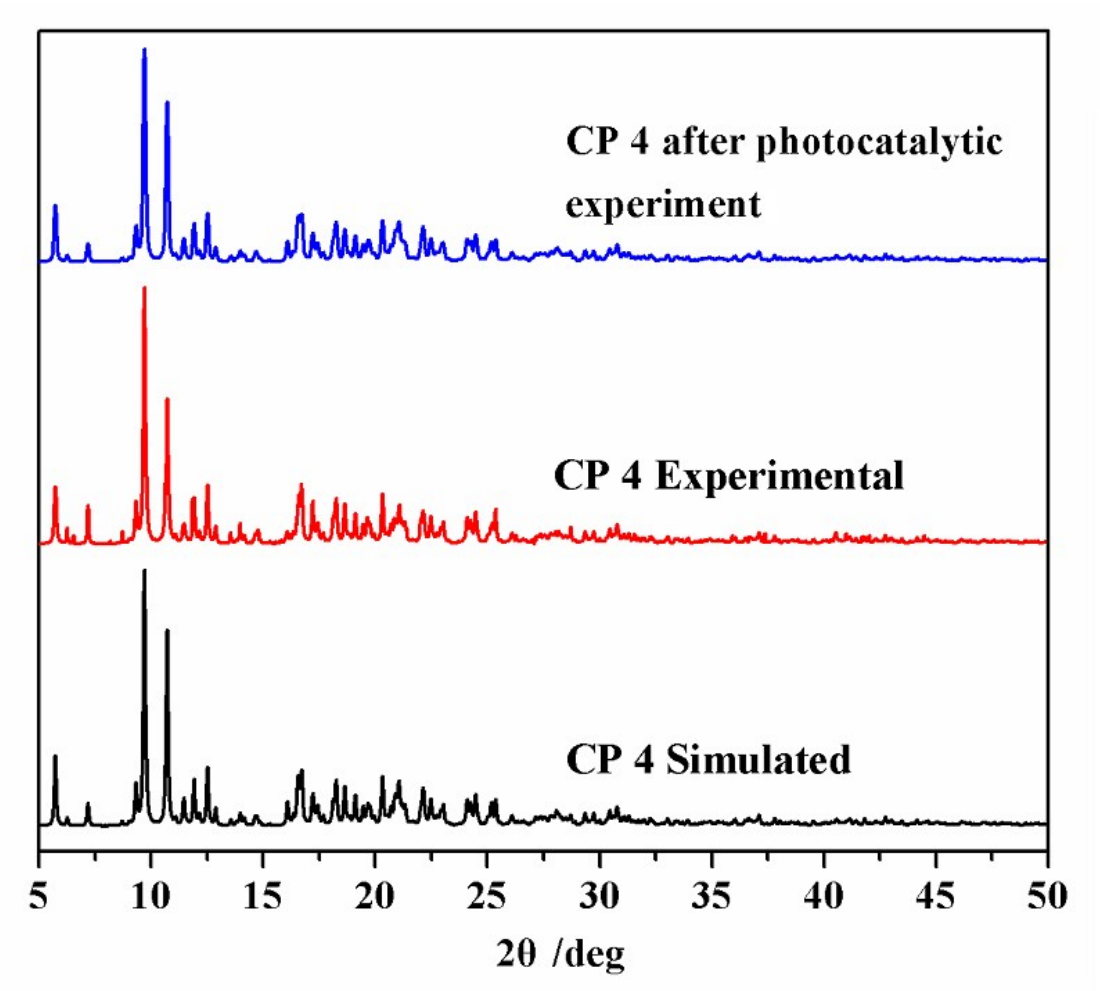
CP 4 after photocatalytic experiment
CP 4 Experimental
CP 4 Simulated
5
10
15
20
25
30
35
40
45
50
2θ /deg

(d)

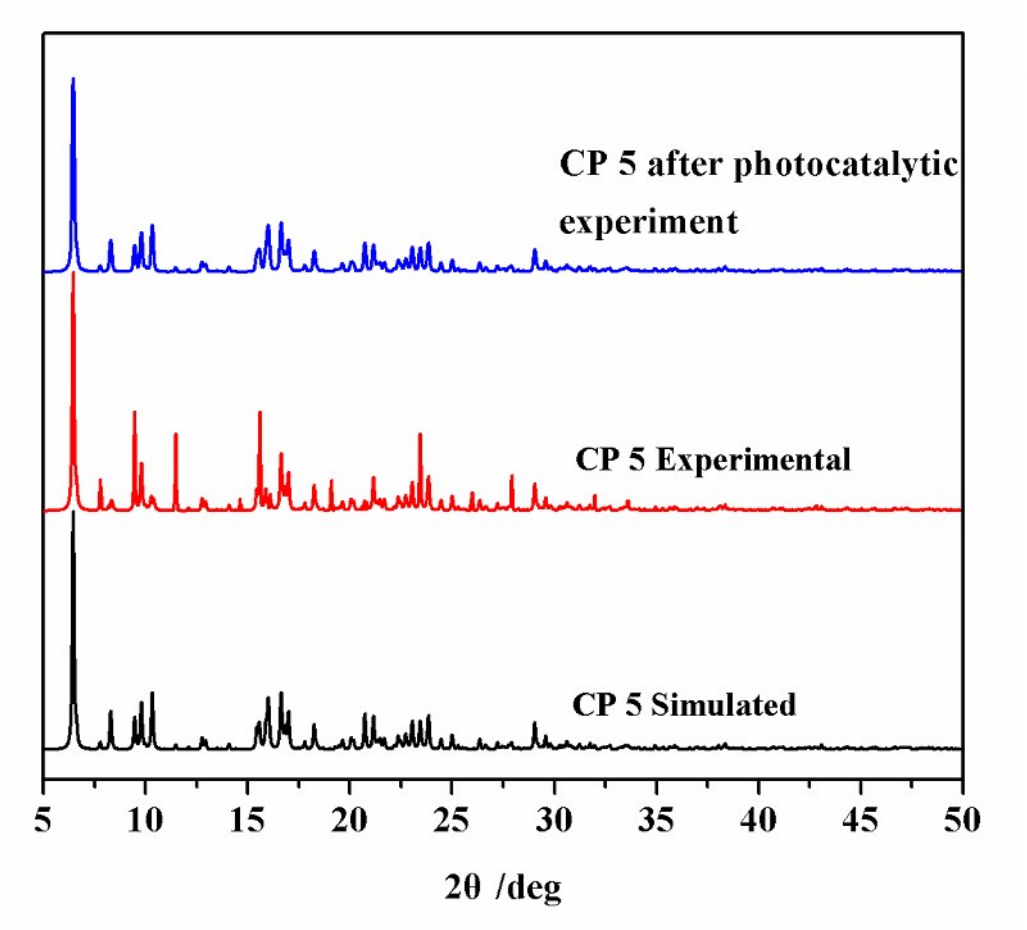
CP 5 after photocatalytic experiment
CP 5 Experimental
CP 5 Simulated
5
10
15
20
25
30
35
40
45
50
2θ /deg

(e)

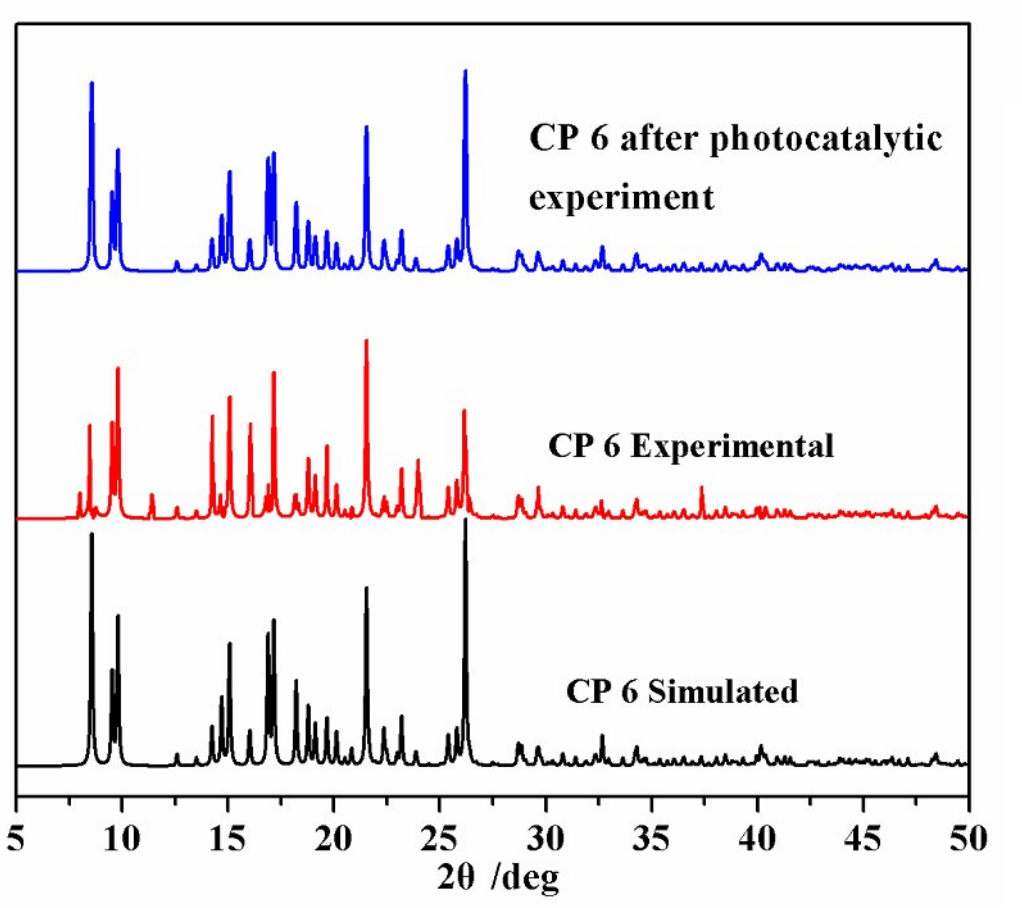

(f)

Fig. S6 X-ray powder diffraction patterns of CPs **1**–**6** after catalytic experiments.

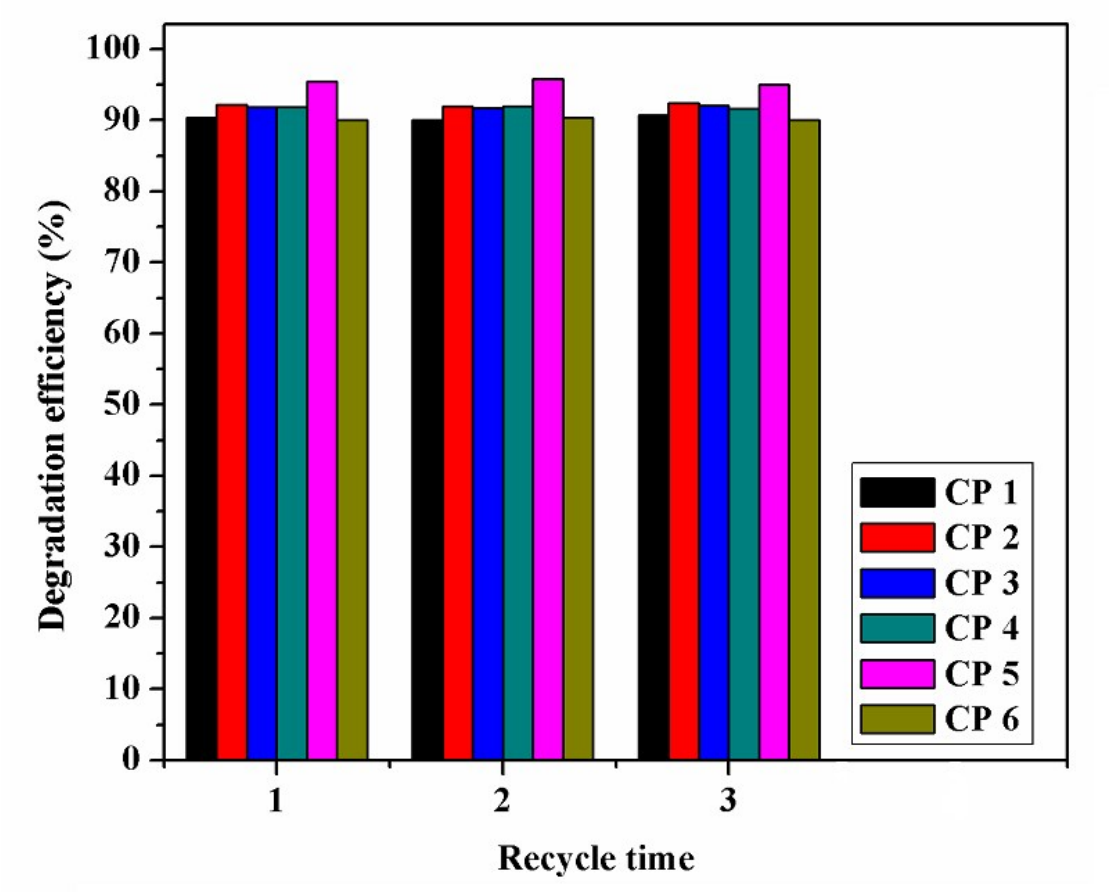

Fig. S7 Three cycling runs of CPs **1**–**6** in the degradation of MB solution.